Muon Capture in Oxygen-16†

VINCENT GILLET* AND DAVID A. JENKINS
Lawrence Radiation Laboratory, University of California, Berkeley, California
(Received 24 May 1965)

The muon capture rate in oxygen is used as a means for measuring the induced pseudoscalar coupling constant (C_P) of weak interactions. The capture rate between the $J^P=0^+$ ground state of O^{16} and the 0^-, 1^-, 2^-, and 3^- states of N^{16} are calculated as a function of C_P with different nuclear models. Using the experimental values of the transition rates, we then determine C_P. We find that the transition rate, and therefore C_P, depends strongly on the nuclear model. We conclude that $5<C_P/C_A<20$.

I. INTRODUCTION

THE muon-capture interaction has gained attention because of the information which it can provide about the weak interaction. The high-momentum transfer available in muon capture makes the reaction sensitive to terms in the weak-interaction Hamiltonian which are not observable in beta decay. Unfortunately, few definite conclusions can be made at present because of uncertainties in either the experiment or the interpretation of the experiment.

We propose to compute the muon capture rate in O^{16},

$$\mu^-+O^{16}\rightarrow N^{16}+\nu, \tag{1}$$

leading to the bound states of N^{16}, and we will examine the sources of ambiguity in the calculation. Several authors have examined this problem. Blokhintsev and Shapiro[1] originally suggested that the capture rate into the $J^P=0^-$ excited state provides a measurement of C_P, the induced pseudoscalar coupling constant of weak interactions. Ericson, Sens, and Rood repeated the calculation and demonstrated that higher order terms must be included.[2] Duck[3] has also done this calculation with the same assumption as Ericson *et al.*, but he obtained a different result for one of the rates.

The experimental results are summarized in Table I.[4,5] Figure 1 shows the four bound states in N^{16} to which capture can occur from the ground state of O^{16}. The spin and parity of these levels are $J^P=0^-$, 1^-, 2^-, and 3^-. The calculated capture rates into the 0^- and 2^- states depend strongly on C_P, but the rates into the 1^- and 3^- levels are independent of C_P. As a result, the 0^- and 2^- capture rates provide a measurement of C_P, and the 1^- and 3^- rates should provide a test for other parts of the calculation.

II. METHOD OF CALCULATION

We begin our analysis with the Hamiltonian introduced by Weinberg,[6]

$$\begin{aligned}\mathcal{H}=&(\bar{\psi}_\nu\gamma_\lambda\psi_l)\bar{\psi}_n[C_V\gamma_\lambda-iC_M\sigma_{\lambda\mu}p_\mu+iC_S(p_\lambda/m_\mu)]\psi_p\\&+(\bar{\psi}_\nu i\gamma_\lambda\gamma_5\psi_l)\bar{\psi}_n[iC_A\gamma_\lambda\gamma_5-C_P(p_\lambda/m_\mu)\gamma_5\\&-C_T\sigma_{\lambda\mu}\gamma_5(p_\mu/W_0)]\psi_p,\end{aligned} \tag{2}$$

where C_V is the vector coupling constant given by beta decay, C_M is found by comparing the weak current with the electromagnetic current, C_S is an "induced scalar" coupling constant (which has not been observed), C_A is the axial-vector coupling constant obtained from beta decay, C_P is the pseudoscalar coupling constant, C_T is the "induced tensor" coupling constant (which has not been observed), and W_0 is the energy difference between the initial and final nuclear states. The Goldberger-Treiman relation predicts a value of about 7 for C_P. Taylor estimated the corrections from high-mass states, and he concluded that C_P must be between 6.5 and 7.5 if the Goldberger-Treiman relation is valid.[7]

Morita and Fujii use the above Hamiltonian to express the capture rate in a spherical tensor form.[8] We have adopted their notation, and throughout our work we have used their reduction of the muon-capture problem.

The lepton part of the interaction is treated relativistically by expanding the plane-wave neutrino in a

TABLE I. Experimental values of the transition rates.

Transition	Berkeley[a] (10^3 sec^{-1})	Columbia[b] (10^3 sec^{-1})
0^-	1.6±0.2	1.1 ±0.2
1^-	1.4±0.2	1.88±0.10[c]
2^-	Not observed	6.3 ±0.7
3^-	Not observed	Not observed

[a] Reference 4.
[b] Reference 5.
[c] The number given in Ref. 5 has been multiplied by 0.75/0.69 = 1.09 to agree with Ref. 4 which uses a $1^-\rightarrow 0^-$ gamma branching ratio of 0.69.

† Work done under auspices of the U. S. Atomic Energy Commission.
* Present address: Centre D'Etudes Nucléaires, Saclay, France.
[1] I. S. Shapiro and L. D. Blokhintsev, Zh. Eksperim. i Teor. Fiz. **39**, 1112 (1960) [English transl.: Soviet Phys.—JETP **12**, 775 (1961)].
[2] T. Ericson, J. C. Sens, and H. P. C. Rood, Nuovo Cimento **34**, 51 (1964); see also H. P. C. Rood, thesis, University of Groningen, Netherlands, 1964 (unpublished).
[3] I. Duck, Ph.D. thesis, California Institute of Technology, 1961; Nucl. Phys. **35**, 27 (1962).
[4] A. Astbury, L. B. Auerbach, D. Cutts, R. J. Esterling, D. A. Jenkins, N. H. Lipman, and R. E. Shafer, Nuovo Cimento **33**, 1020 (1964).
[5] R. Cohen, S. Devons, and A. Kanaris, Phys. Rev. Letters **11**, 134 (1963); also Nucl. Phys. **57**, 255 (1964).
[6] S. Weinberg, Phys. Rev. **112**, 1375 (1958).
[7] J. C. Taylor, Phys. Letters **11**, 77 (1964).
[8] M. Morita and A. Fujii, Phys. Rev. **118**, 606 (1960).

spherical representation in terms of spinors with a definite angular momentum κ,

$$l=\kappa, \quad j=l-\tfrac{1}{2} \text{ for } \kappa>0,$$
$$l=-\kappa-1, \quad j=l+\tfrac{1}{2} \text{ for } \kappa<0,$$

and spin projection μ. The radial part of the neutrino wave function is given by

$$g_\kappa=\pi^{-1/2}j_l(qr),$$
$$f_\kappa=\pi^{-1/2}S_\kappa j_{\bar{l}}(qr), \tag{3}$$

where S_κ is the sign of κ, $j_l(qr)$ is a spherical Bessel function, l is the orbital momentum corresponding to κ, and $\bar{l}$ is the orbital momentum corresponding to $-\kappa$. The muon wave function is treated in the same representation, but it has a simple form, since the muon is assumed to be capture from the $1s_{1/2}$ orbit:

$$G_{-1}=(2Z/a_0)^{3/2}[(1+\gamma)/2\Gamma(2\gamma+1)]^{1/2} \times\exp(-Zr/a_0)(2Zr/a_0)^{\gamma-1}, \tag{4}$$
$$F_{-1}=-[(1-\gamma)/(1+\gamma)]^{1/2}G_{-1},$$

where

$$\gamma=[1-(\alpha Z)^2]^{1/2}$$

and F_{-1} is referred to as the relativistic component of the muon wave function. These wave functions are for a point nucleus. The calculation is easily adapted to a finite nucleus by means of the wave functions of Ref. 9 or 10, but the correction is probably unimportant compared with the other uncertainties in the problem. Flamand and Ford[11] found that the muon-capture rate in carbon was 6% less for a finite nucleus than for a point nucleus, and the effect in O^{16} could reduce the capture rate by as much as 10%.[12]

The angular momenta (j) of the muon and neutrino are coupled to a total spin u, and the orbital angular momenta (l) are coupled to a total spin v. In this representation, selection rules can be used for the nuclear transition. By conservation of angular momentum, one has

$$|J_i-J_f|\leqslant u\leqslant|J_i+J_f|.$$

For O^{16}, $J_i=0$, then $u=J_f$ and the lepton system has a definite spin.

The transiton rate from the ground state $|0\rangle$ of spin $J_i=0$ to the excited state $|f\rangle$ of spin J_f and excitation energy $W_0(W_0=E_f-E_0)$ is given by

$$\lambda=2\pi|\langle f|H|0\rangle|_{\mathrm{av}}{}^2q^2dq/dE, \tag{5}$$

with units $\hbar=c=m_e=1$, where the matrix element is averaged over the initial states and summed over final states, q is the momentum of the neutrino, and dq/dE is a density-of-states factor,

$$dq/dE=1-q/(m_\mu+AM). \tag{6}$$

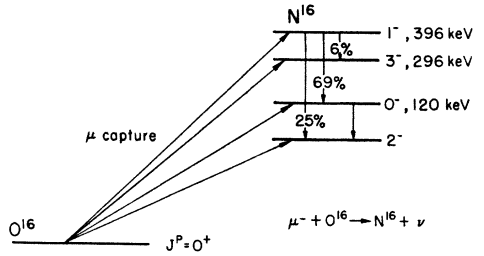

FIG. 1. Level scheme for the muon-capture reaction in O^{16}.

The expression $\langle f|H|0\rangle$ is given by Morita-Fujii in terms of the reduced nuclear-matrix elements $\mathfrak{M}_{vu}{}^{(i)}(\kappa)$ and the coupling constants $C^{(i)}$,

$$|\langle f|H|0\rangle|_{\mathrm{av}}{}^2=\tfrac{1}{2}(2J_f+1)\sum_{i,j}\sum_{\kappa}C^{(i)}C^{(j)} \times[\sum_{v}\mathfrak{M}_{vu}{}^{(i)}(\kappa)][\sum_{v'}\mathfrak{M}_{v'u}{}^{(j)}(\kappa)], \tag{7}$$

where

$$\mathfrak{M}_{vu}{}^{(i)}(\kappa)=(2J_f+1)^{-1/2}\langle f\|\Xi^{(i)}\|0\rangle \tag{8}$$

is a one-body matrix element between states $|0\rangle$ and $|f\rangle$. The terms $\Xi^{(i)}$ are listed in Table II with the coupling constants $C^{(i)}$ as given by Morita-Fujii.[8] New entries in this table for the induced scalar (C_S) and induced tensor (C_T) couplings have been computed by Morita and Morita.[13] In our calculations we have used the following values for the coupling constants:

$$C_A{}^\beta=-1.18C_V{}^\beta,$$
$$C_V=0.972C_V{}^\beta,$$
$$C_A=0.999C_A{}^\beta,$$
$$C_V{}^\beta=1.015\times10^{-5}/M^2,$$
$$C_M=3.706C_V/2M,$$
$$C_S=0,$$
$$C_T=0,$$

where M is the proton mass. The term C_P is treated as a free parameter. If the vector and axial-vector currents behave properly under G conjugation, C_S and C_T are equal to zero. With our limited amount of data, we must make this assumption to simplify the calculation of C_P. However, Cabibbo has shown that the CP violation recently found in $K_2{}^0$ decay may indicate that these terms are not zero.[14]

The nuclear integration for the reduced matrix elements between states p and h gives (we use the phases

[9] K. W. Ford and J. G. Wills, Los Alamos Scientific Laboratory Report LAMS-2387, 1960 (unpublished); Nucl. Phys. 35, 295 (1962).
[10] G. E. Pustovalov, Zh. Eksperim. i Teor. Fiz. 36, 1806 (1959) [English transl.: Soviet Phys.—JETP 9, 1288 (1959)].
[11] G. Flamand and K. W. Ford, Phys. Rev. 116, 1591 (1959).
[12] We thank Dr. Kenneth W. Ford for a discussion on this point.
[13] M. Morita and R. Morita, J. Phys. Soc. Japan 19, 1759 (1964).
[14] N. Cabibbo, Phys. Letters 12, 137 (1964).

TABLE II. Coupling constants $C^{(i)}$ and operators $\Xi^{(i)}$ in Eqs. (7) and (8). Subscript s refers to nuclear variables.

i	$C^{(i)}$	Ξ
1	C_V	$\mathfrak{D}_{0vu}{}^{Mf-Mi}(\hat{r}_s)[g_\kappa G_{\kappa'} S_{0vu}(\kappa,\kappa') - f_\kappa F_{\kappa'} S_{0vu}(-\kappa,-\kappa')]\delta_{vu}$
2	$-C_A+C_T$	$\mathfrak{D}_{1vu}{}^{Mf-Mi}(\hat{r}_s,\boldsymbol{\sigma}_s)[g_\kappa G_{\kappa'} S_{1vu}(\kappa,\kappa') - f_\kappa F_{\kappa'} S_{1vu}(-\kappa,-\kappa')]$
3	$-C_V/M$	$i[f_\kappa G_{\kappa'} S_{1vu}(-\kappa,\kappa') + g_\kappa F_{\kappa'} S_{1vu}(\kappa,-\kappa')]\mathfrak{D}_{1vu}{}^{Mf-Mi}(\hat{r}_s,\mathbf{p}_s)$
4	$-\sqrt{3}C_V/2M$	$\{[(v+1)/(2v+3)]^{1/2}\mathfrak{D}_{0v+1u}{}^{Mf-Mi}(\hat{r}_s)\delta_{v+1u}D_+ - [v/(2v-1)]^{1/2}\mathfrak{D}_{0v-1u}{}^{Mf-Mi}(\hat{r}_s)\delta_{v-1u}D_-\}$ $\times[f_\kappa G_{\kappa'} S_{1vu}(-\kappa,\kappa') + g_\kappa F_{\kappa'} S_{1vu}(\kappa,-\kappa')]$
5	$-(\frac{3}{2})^{1/2}C_V(1+\mu_p-\mu_n)/M$	$[(v+1)^{1/2}W(11uv,1v+1)\mathfrak{D}_{1v+1u}{}^{Mf-Mi}(\hat{r}_s,\boldsymbol{\sigma}_s)D_+ - v^{1/2}W(11uv,1v-1)\mathfrak{D}_{1v-1u}{}^{Mf-Mi}(\hat{r}_s,\boldsymbol{\sigma}_s)D_-]$ $\times[f_\kappa G_{\kappa'} S_{1vu}(-\kappa,\kappa') + g_\kappa F_{\kappa'} S_{1vu}(\kappa,-\kappa')]$
6	C_A/M	$i\mathfrak{D}_{0vu}{}^{Mf-Mi}(\hat{r}_s)[f_\kappa G_{\kappa'} S_{0vu}(-\kappa,\kappa') + g_\kappa F_{\kappa'} S_{0vu}(\kappa,-\kappa')]\boldsymbol{\sigma}_s\cdot\mathbf{p}_s$
7	$-(\sqrt{3})^{-1}[C_A/2M - C_T/W_0]$	$\{[(v+1)/(2v+1)]^{1/2}\mathfrak{D}_{1v+1u}{}^{Mf-Mi}(\hat{r}_s,\boldsymbol{\sigma}_s)D_+ - [v/(2v+1)]^{1/2}\mathfrak{D}_{1v-1u}{}^{Mf-Mi}(\hat{r}_v,\boldsymbol{\sigma}_s)D_-\}$ $\times[f_\kappa G_{\kappa'} S_{0vu}(-\kappa,\kappa') \pm g_\kappa F_{\kappa'} S_{0vu}(\kappa,-\kappa')]\delta_{vu}$
8	$C_P/2\sqrt{3}M$	
9	C_S	$\mathfrak{D}_{0vu}{}^{Mf-Mi}(\hat{r}_s)[g_\kappa G_{\kappa'} S_{0vu}(\kappa,\kappa') + f_\kappa F_{\kappa'} S_{0vu}(-\kappa,-\kappa')]\delta_{vu}$

of Edmonds[15])

$$\left.\begin{matrix}\langle p\|\Xi^{(1)}\|h\rangle \\ \langle p\|\Xi^{(9)}\|h\rangle\end{matrix}\right\} = \langle l_p\|\mathfrak{D}_{0vu}(\hat{r})\|l_h\rangle\int_0^\infty u_p[g_\kappa G_{\kappa'} S_{0vu}(\kappa,\kappa') \mp f_\kappa F_{\kappa'} S_{0vu}(-\kappa,-\kappa')]u_h r^2 dr\,,$$

where the $-$ sign refers to $i=1$ and the $+$ sign to $i=9$:

$$\langle p\|\Xi^{(2)}\|h\rangle = \langle l_p\|\mathfrak{D}_{1vu}(\hat{r},\boldsymbol{\sigma})\|l_h\rangle\int_0^\infty u_p[g_\kappa G_{\kappa'} S_{1vu}(\kappa,\kappa') - f_\kappa F_{\kappa'} S_{1vu}(-\kappa,-\kappa')]u_h r^2 dr\,.$$

$$\langle p\|\Xi^{(3)}\|h\rangle = (-)^{3/2+j_h+l_h+l_p+v-u}(\sqrt{3}/4\pi)\hat{j}_p\hat{j}_h\hat{u}\hat{l}_p\hat{v}\begin{Bmatrix} l_p & j_p & 1/2 \\ j_h & l_h & u\end{Bmatrix}\sum_{l'=l_h\pm1} l'\begin{Bmatrix} v & 1 & u \\ l_h & l_p & l'\end{Bmatrix}\begin{pmatrix} l_p & v & l' \\ 0 & 0 & 0\end{pmatrix}$$

$$\times\int u_p[f_\kappa G_{\kappa'} S_{1vu}(-\kappa,\kappa') + g_\kappa F_{\kappa'} S_{1vu}(\kappa,-\kappa')]D_{l'}u_h r^2 dr\,,$$

where

$$D_{l'} = (-)^{l_h}\sqrt{3}(l_h+1)(d/dr - l_h/r)/[(2l_h+1)(2l_h+3)]^{1/2}(l'l_h00|10) \quad \text{if} \quad l'=l_h+1$$

and

$$D_{l'} = (-)^{l_h}\sqrt{3}l_h[d/dr + (l_h+1)/r]/[(2l_h-1)(2l_h+1)]^{1/2}(l'l_h00|10) \quad \text{if} \quad l'=l_h-1$$

are operators that act on u_a:

$$\langle p\|\Xi^{(4)}\|h\rangle = [(v+1)/(2v+3)]^{1/2}\langle l_p\|\mathfrak{D}_{0v+1u}(\hat{r})\|l_h\rangle\delta_{v+1,u}\int_0^\infty u_p D_+[f_\kappa G_{\kappa'} S_{1vu}(-\kappa,\kappa') + g_\kappa F_{\kappa'} S_{1vu}(\kappa,-\kappa')]u_h r^2 dr$$

$$-[v/(2v-1)]^{1/2}\langle l_p\|\mathfrak{D}_{0v-1u}(\hat{r})\|l_h\rangle\delta_{v-1,u}\int_0^\infty u_p D_-[f_\kappa G_{\kappa'} S_{1vu}(-\kappa,\kappa') + g_\kappa F_{\kappa'} S_{1vu}(\kappa,-\kappa')]u_h r^2 dr\,,$$

where

$$D_+ = d/dr - v/r \quad \text{and} \quad D_- = d/dr + (v+1)/r$$

are operators that act only on the lepton wave functions:

$$\langle p\|\Xi^{(5)}\|h\rangle = (v+1)^{1/2}W(11uv,1v+1)\langle l_p\|\mathfrak{D}_{1v+1u}(\hat{r},\boldsymbol{\sigma})\|l_h\rangle\int_0^\infty u_p D_+[f_\kappa G_{\kappa'} S_{1vu}(-\kappa,\kappa') + g_\kappa F_{\kappa'} S_{1vu}(\kappa,-\kappa')]u_h r^2 dr$$

$$-v^{1/2}W(11uv,1v-1)\langle l_p\|\mathfrak{D}_{1v-1u}(\hat{r},\boldsymbol{\sigma})\|l_h\rangle\int_0^\infty u_p D_-[f_\kappa G_{\kappa'} S_{1vu}(-\kappa,\kappa') + g_\kappa F_{\kappa'} S_{1vu}(\kappa,-\kappa')]u_h r^2 dr$$

[15] A. R. Edmonds, *Angular Momentum in Quantum Mechanics* (Princeton University Press, Princeton, New Jersey, 1957).

$$\langle p\|\Xi^{(6)}\|h\rangle=(-)^{l_h+j_h+1/2}(6)^{1/2}\sum_{l'=l_h\pm1}\langle l_p\|\mathfrak{D}_{0vu}(\hat{r})\|l'\rangle\begin{Bmatrix}j_h & 1/2 & l'\\ 1 & l_h & 1/2\end{Bmatrix}$$
$$\times\int_0^\infty u_p[f_\kappa G_{\kappa'}S_{0vu}(-\kappa,\kappa')+g_\kappa F_{\kappa'}S_{0vu}(\kappa,-\kappa')]D_{l'}u_h r^2dr,$$

$$\begin{Bmatrix}\langle p\|\Xi^{(7)}\|h\rangle\\ \langle p\|\Xi^{(8)}\|h\rangle\end{Bmatrix}=\left(\frac{v+1}{2v+1}\right)^{1/2}\langle l_p\|\mathfrak{D}_{1v+1u}(\hat{r},\boldsymbol{\sigma})\|l_h\rangle\delta_{vu}\int_0^\infty u_pD_+[f_\kappa G_{\kappa'}S_{0vu}(-\kappa,\kappa')\pm g_\kappa F_{\kappa'}S_{0vu}(\kappa,-\kappa')]u_hr^2dr$$
$$-[v/(2v+1)]^{1/2}\langle l_p\|\mathfrak{D}_{1v-1u}(\hat{r},\boldsymbol{\sigma})\|l_h\rangle\delta_{vu}\int_0^\infty u_pD_-[f_\kappa G_{\kappa'}S_{0vu}(-\kappa,\kappa')\pm g_\kappa F_{\kappa'}S_{0vu}(\kappa,-\kappa')]u_hr^2dr,$$

where the + sign refers to $i=7$ and the − sign to $i=8$. The symbols p and h indicate the lsj quantum numbers for the respective state. Here u_p and u_h are harmonic-oscillator wave functions,

$$u_{n,l}(r)=Nb^{-l-3/2}P(r)r^le^{-1/2(r/b)^2},$$

where N is a normalization constant

$$N=(1/\pi^{1/4})[2^{n+l+1}/(2n+2l-1)!!]^{1/2},$$

b is the oscillator-length parameter, and

$$\begin{aligned}P(r)&=1 && \text{for } n=1,\\ &=\tfrac{1}{2}(2l+1)-(r/b)^2 && \text{for } n=2,\\ &=\tfrac{1}{2}[\tfrac{1}{4}(2l+3)(2l+5)-(2l+5)(r/b)^2+(r/b)^4] && \text{for } n=3.\end{aligned}$$

We use the reduced matrix elements

$$\langle l_p\|\mathfrak{D}_{0vu}(\hat{r})\|l_h\rangle=\frac{(-)^{1/2+j_h+u}}{4\pi}\hat{j}_h\hat{j}_p\hat{l}_p\hat{l}_h\hat{u}\begin{Bmatrix}l_p & j_p & 1/2\\ j_h & l_h & u\end{Bmatrix}\begin{pmatrix}l_p & u & l_h\\ 0 & 0 & 0\end{pmatrix},$$

$$\langle l_p\|\mathfrak{D}_{1vu}(\hat{r},\boldsymbol{\sigma})\|l_h\rangle=(-)^{1+v+l_p-u}(3/2\sqrt{2}\pi)\hat{l}_p\hat{l}_h\hat{v}\hat{j}_h\hat{j}_p\hat{u}\begin{pmatrix}l_p & v & l_h\\ 0 & 0 & 0\end{pmatrix}\begin{Bmatrix}l_p & l_h & v\\ 1/2 & 1/2 & 1\\ j_p & j_h & u\end{Bmatrix},$$

$$S_{kvu}(\kappa,\kappa')=\sqrt{2}\hat{l}\hat{l}'\hat{j}\hat{j}'(ll'00|v0)\begin{Bmatrix}l & l' & v\\ j & j' & u\\ 1/2 & 1/2 & k\end{Bmatrix},$$

where $\hat{j}\equiv(2j+1)^{1/2}$, and we have set $\kappa'=-1$.

III. NUCLEAR WAVE FUNCTIONS

A calculation of C_P requires a good knowledge of the nuclear wave function. The purpose of our work is to determine the uncertainty in the computation of C_P due to uncertainties of the nuclear wave functions coming from the nuclear problem itself, which is only approximately solved. Three nuclear models are used:

(a) the independent-particle model (IP),

(b) the diagonalization of the residual interaction in the subspace of the $1\hbar\omega$ particle-hole excitations (approximation I),

(c) the random-phase approximation (RPA) (approximation II).

The particle-hole wave function of the excited state is of the form

$$|f\rangle=\sum_{m_pm_h}X_{\mathrm{ph}}{}^{J_f}(j_pj_hm_pm_h|J_fM)\xi_{pm_p}{}^\dagger\xi_{hm_h}{}^\dagger|0\rangle. \quad (9)$$

The ket $|0\rangle$ is the Hartree-Fock ground state and the $X_{ph}{}^J$ are the configuration mixing amplitudes associated with the particle-hole configurations (ph). Their normalization is

$$\sum_{ph}(X_{ph}{}^J)^2=1.$$

The associated "quasiparticle" operators $\xi^\dagger$, ξ are related to the true particle operators $\eta^\dagger$, η through the

transformation[16]

$$\xi_{pm_p}{}^{\dagger}=\eta_{pm_p}{}^{\dagger},$$
$$\xi_{hm_h}{}^{\dagger}=(-)^{j_h+m_h}\eta_{h-m_h}.$$

We have used particle-hole amplitudes computed by two different groups, and we must therefore be careful to use the proper phase conventions. In Ref. 17 the tabulated amplitudes $X_{ph}{}^{J}$ differ from the above choice of phases by a factor $(-)^{j_h+1/2}$. The phases of Elliott and Flowers[18] differ from the above because of their use of (i) the Condon and Shortley convention for the spin and orbital-angular-momentum coupling order (slj), (ii) a $2s$ harmonic-oscillator wave function which is negative near the origin, and (iii) the opposite coupling order in their particle-hole amplitudes.

The one-body operator for absorption of a multipole radiation λ, accompanied by the jump of a nucleon from the single-particle state α to state β, is

$$\Xi_{\mu}{}^{\lambda}=\sum_{\alpha\beta}\frac{\langle\alpha\|\Xi^{\lambda}\|\beta\rangle}{(2\lambda+1)^{1/2}}(-)^{j_\beta-m_\beta}\times(j_\alpha j_\beta m_\alpha -m_\beta|\lambda\mu)\eta_{\alpha m_\alpha}{}^{\dagger}\eta_{\beta m_\beta}, \quad (10)$$

where $\langle\alpha\|\Xi^{\lambda}\|\beta\rangle$ is a one-body reduced matrix element.

With the definitions (9) and (10) the transition matrix element in approximation I is

$$\langle f|\Xi_{\mu}{}^{\lambda}|0\rangle=\delta_{J_f\lambda}\delta_{M\mu}\sum_{ph}X_{ph}{}^{J_f}\frac{\langle p\|\Xi^{J_f}\|h\rangle}{(2J_f+1)^{1/2}}.$$

This expression reduces to one term in the independent-particle model (IP), for which $X_{ph}=1$.

In approximation II (RPA), one has also to take into account the probability amplitude $Y_{ph}{}^{J}$ for exciting the nuclear state $|f,J_fM\rangle$ by annihilation of a particle-hole pair (ph) in the ground state. The expression for the transition matrix element is then

$$\langle f|\Xi_{\mu}{}^{\lambda}|0\rangle=\delta_{J_f\lambda}\delta_{M\mu}(2J_f+1)^{-1/2}\sum_{ph}\{X_{ph}{}^{J_f}\langle p\|\Xi^{J_f}\|h\rangle+Y_{ph}{}^{J_f}\langle h\|\Xi^{J_f}\|p\rangle\}.$$

The normalization of the amplitudes in this case is

$$\sum_{ph}\{(X_{ph}{}^{J})^2-(Y_{ph}{}^{J})^2\}=1.$$

Then the reduced matrix elements of Eq. (8) are given by

$$\langle f\|\Xi^{(i)}\|0\rangle=\sum_{ph}X_{ph}{}^{J_f}\langle p\|\Xi^{(i)}\|h\rangle+Y_{ph}{}^{J_f}\langle h\|\Xi^{(i)}\|p\rangle. \quad (11)$$

The wave functions for the N^{16} bound states are taken from the wave functions for the analogous levels in O^{16} under the assumption of good isospin.

In approximation I we use wave functions derived from two different potentials. The first potential is the Rosenfeld mixture used by Elliott and Flowers,[18] and the second potential is found from a least-squares search carried over nine energy levels of O^{16} by Gillet and Vinh Mau.[19] Wave functions are derived from the potentials by finding the set of basis vectors ψ for which the matrix $\langle\psi_\alpha|V|\psi_\beta\rangle$ is diagonal. Since two values of the potential V were used in these two analyses, two different wave functions are obtained. Both potentials, with strongly different characteristics as seen from Table III, give similar over-all good fits for the energies. However, the different potentials affect the small components of the nuclear wave function appreciably, as shown in Table IV, allowing a numerical discussion of the uncertainties due to the nuclear parameters.

For the purpose of this paper, it is important to note in Table IV the difference in sign of the small component of the 0^- wave function for the two cases in approximation I. As will be shown later, the capture rate and the value of C_P are very sensitive to this component. We have a preliminary report of a third calculation of the 0^- wave function made by Lewis.[20] He obtains an amplitude of -0.07 for the $1p_{-3/2}(1d_{3/2})$ component of the 0^- wave function as compared with Gillet's amplitude of $+0.055$. However, Lewis used a Serber force, and this would be expected to give a somewhat different result.

IV. RESULTS

The reduced matrix elements $\mathfrak{M}_{\nu u}{}^{(i)}$ were calculated on an IBM-7094 computer to allow the use of numerical methods to evaluate the radial integrals. In checking our method, we first calculated the muon-capture rate in C^{12} to the ground state of B^{12} in order to compare our result with the Morita and Fujii calculation.[8] Because of ambiguities in the nuclear wave function, the computed capture rate does not agree with the rate determined experimentally. Morita and Fujii correct this by taking a ratio with the inverse-

TABLE III. Nuclear potential used in calculating O^{16} wave functions.[a]

	V(MeV)	μ/b	H	θ	η
Elliott and Flowers[b]	−40	0.90	−0.26	1.06	0.6
Gillet[c]	−40	1.0	0.4	0	0.4

[a] In this table the potential is defined by $V(r)=f(r/\mu)V(W+BP\sigma-HP\gamma+MP\sigma P\gamma)$; $P\sigma$ and $P\gamma$ are spin and isobaric-spin exchange operators, $f(r/\mu)$ is a radial form factor, V is the potential depth, W, B, H, and M are the four exchange coefficients, b is the oscillator-length parameter, and μ is the range of the force, $\theta=M-W$, and $\eta=M+W-B-H$.
[b] Reference 18.
[c] Reference 17.

[16] J. S. Bell, Nucl. Phys. **12**, 117 (1959).
[17] Vincent Gillet, Ph.D. thesis, Centre d'Etudes Nucléaires de Saclay Rapport CEA-2177, 1962 (unpublished); Nucl. Phys. **51**, 410 (1964).
[18] J. P. Elliott and B. H. Flowers, Proc. Roy. Soc. (London) **A242**, 57 (1957).
[19] V. Gillet and N. Vinh Mau, Nucl. Phys. **54**, 321 (1964). See also Erratum, Nucl. Phys. **57**, 698 (1964).
[20] F. H. Lewis (private communication).

TABLE IV. The wave-function amplitudes X and Y for O^{16} as given by the particle-hole models. Case I_A is taken from Ref. 18, cases I_B and II are taken from Ref. 17, and the phases have been modified to be consistent with the convention of Eq. (9). In approximation II, the X and Y amplitudes are given in that order.

N^{16} state	Model	$1p_{-1/2}$ $2s_{1/2}$	$1p_{-1/2}$ $1d_{5/2}$	$1p_{-1/2}$ $1d_{3/2}$	$1p_{-3/2}$ $2s_{1/2}$	$1p_{-3/2}$ $1d_{5/2}$	$1p_{-3/2}$ $1d_{3/2}$	$2s_{-1/2}$ $1p_{1/2}$	$1d_{-5/2}$ $1p_{1/2}$	$1d_{-3/2}$ $1p_{1/2}$	$2s_{-1/2}$ $1p_{3/2}$	$1d_{-5/2}$ $1p_{3/2}$	$1d_{-3/2}$ $1p_{3/2}$
0^-	IP	1.00	...	...	...	...	...	...	...	...	...	...	...
	I_A	1.00	...	...	...	...	−0.05	...	...	...	...	...	...
	I_B	0.999	...	...	...	...	0.055	...	...	...	...	...	...
	II	0.99	...	...	...	...	0.053	−0.012	...	...	...	...	0.012
1^-	IP	1.00	...	...	...	...	...	...	...	...	...	...	...
	I_A	0.98	...	0.01	−0.16	−0.08	−0.02	...	...	...	...	...	...
	I_B	0.995	...	−0.008	0.026	−0.096	−0.020	...	...	...	...	...	...
	II	0.996	...	−0.006	0.026	−0.090	−0.019	0.001	...	−0.009	−0.012	−0.008	0.008
2^-	IP	...	1.00	...	...	...	...	...	...	...	...	...	...
	I_A	...	0.98	−0.10	0.06	0.14	0.09	...	...	...	...	...	...
	I_B	...	0.983	0.007	0.054	0.174	0.035	...	...	...	...	...	...
	II	...	0.985	0.007	0.051	0.166	0.034	...	−0.026	−0.001	0.009	0.020	0.015
3^-	IP	...	1.00	...	...	...	...	...	...	...	...	...	...
	I_A	...	0.98	...	...	−0.18	0.06	...	...	...	...	...	...
	I_B	...	0.998	...	...	−0.062	−0.011	...	...	...	...	...	...
	II	...	0.999	...	...	−0.059	−0.010	...	0.000	...	...	−0.004	0.029

beta-decay transition, and obtain for the capture rate

$$\lambda_{exp}{}^{\mu} = (\lambda_{calc}{}^{\mu}/\lambda_{calc}{}^{\beta})\lambda_{exp}{}^{\beta}, \quad (12)$$

where $\lambda_{calc}{}^{\mu}$ is the muon-capture rate calculated with the Morita-Fujii method, and λ_{exp} is the observed rate. Using[8]

$$\lambda_{exp}{}^{\beta} = 33.15 \text{ sec}^{-1} \text{ and}$$
$$\lambda_{calc}{}^{\beta} = 159 \text{ sec}^{-1},$$

and an oscillator length parameter $b = 1.59$ F, we obtain the results given in Fig. 2, which shows $\lambda_{exp}{}^{\mu}$ as a function of C_P/C_A and the experimental value of $6750_{-750}{}^{+800}$ sec^{-1} measured by Maier *et al.*[21] From the graph we would conclude $10 < C_P/C_A < 30$, where we have not allowed for errors in the nuclear wave function. The capture rate $\lambda_{calc}{}^{\mu}$ has been computed by Morita with his method in which the relativistic component of the muon wave function is set equal to zero. With the relativistic component, we obtain a transition rate of 35.0×10^3 sec^{-1}, which compares to the value 34.2×10^3 sec^{-1} of Morita and Fujii. This good agreement provides a check on our computer program.

We now compute the transition rates in O^{16}, and in Table V we compare the theoretical transition rates, using the wave functions I_B of Table IV with and without the small relativistic component of the muon wave function. This component has been neglected in earlier calculations. The relativistic component affects the transition rate by only a few percent, which is insignificant when compared with the other sources of uncertainty discussed in the following sections. Nevertheless, the relativistic component is included in the following results.

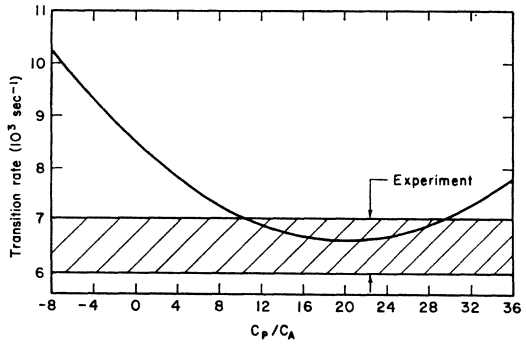

FIG. 2. Muon-capture rate in C^{12}.

[21] E. J. Maier, R. M. Edelstein, and R. T. Siegel, Phys. Rev. 133, B663 (1964).

TABLE V. Effect of neglecting the small relativistic component of the bound-muon wave function. The columns labeled 1 are obtained by using only the large component of the wave function in Eq. (4) and those labeled 2 are obtained by using the complete wave function. The nuclear wave function used is the case I_B, Table IV.

	Transition rate (10^3 sec^{-1})							
	0^-		1^-		2^-		3^-	
C_P/C_A	1	2	1	2	1	2	1	2
−8	4.80	4.73	2.54	2.53	25.7	25.8	0.186	0.196
−4	3.88	3.83			22.6	22.7		
0	3.06	3.01			20.0	20.0		
4	2.33	2.30			17.8	17.8		
8	1.71	1.68			16.0	16.0		
12	1.18	1.16			14.6	14.6		
16	0.749	0.735			13.8	13.7		
20	0.415	0.406			13.3	13.2		
24	0.179	0.174			13.3	13.2		
28	0.0411	0.0392			13.7	13.6		
32	0	0			14.6	14.4		
36	0.0571	0.0584			15.9	15.7		

TABLE VI. Effect of the variation of the oscillator-length parameter. Columns 1, 2, and 3 correspond to $b=1.59$, 1.75, 1.96 F, respectively. The central value is the one obtained from elastic-electron-scattering data. The wave functions used are the ones of case I_B of Table IV.

	Transition rate (10^8 sec^{-1})											
	0^-			1^-			2^-			3^-		
C_P/C_A	1	2	3	1	2	3	1	2	3	1	2	3
−8	5.03	4.73	4.30	2.45	2.53	2.48	23.6	25.8	27.8	0.116	0.196	0.343
−4	4.09	3.83	3.46				20.7	22.7	24.5			
0	3.25	3.01	2.71				18.2	20.0	21.7			
4	2.50	2.30	2.05				16.1	17.8	19.4			
8	1.85	1.68	1.49				14.4	16.0	17.5			
12	1.30	1.16	1.01				13.1	14.6	16.1			
16	0.849	0.735	0.627				12.2	13.7	15.1			
20	0.491	0.406	0.334				11.8	13.2	14.6			
24	0.231	0.174	0.133				11.8	13.2	14.6			
28	0.0679	0.0392	0.0226				12.2	13.6	15.0			
32	0	0	0				12.9	14.4	15.9			
36	0.0323	0.0584	0.0768				14.1	15.7	17.2			

The oscillator-length parameter b that enters into the oscillator-well wave functions is, in principle, given by an analysis of the elastic electron-scattering data, i.e., 1.75 F for O^{16}.[22] In Table VI we show the results of varying the O^{16} oscillator length by 15% while using the wave functions of case I_B. A 10% change in b produces about a 10% change in the 0^- transition rate for $C_P/C_A \approx 8$.

The transition rates for different nuclear models and $b=1.75$ F are tabulated in Table VII. As one would expect for the almost pure states considered here, the transition computed with approximation II (RPA) and approximation I_B differ only slightly, as shown in columns I_B and II. The agreement in the 2^- and 3^- transition rates for the I_A and I_B wave functions shows that these rates are not very sensitive to the small components of the nuclear wave functions, which are rather different (Table IV).

In Fig. 3 we show the 0^- transition rate as a function of C_P for three nuclear models. The wave functions for the three cases are given by

$$\psi_{IP}=|1p_{-1/2}2s_{1/2}\rangle,$$
$$\psi_A=0.99|1p_{-1/2}2s_{1/2}\rangle-0.05|1p_{-3/2}1d_{3/2}\rangle,$$
$$\psi_B=0.99|1p_{-1/2}2s_{1/2}\rangle+0.055|1p_{-3/2}1d_{3/2}\rangle,$$

where ψ_{IP} represents the independent-particle model, ψ_A is the Elliott and Flowers wave function, and ψ_B is the Gillet and Vinh Mau wave function. The only difference between ψ_A and ψ_B is in the sign of the small component of the wave function. As shown in Fig. 3, a variation in the small component produces large differences in the 0^- transition rate. The sensitivity of the transition rates to the small component is to be expected, since the small amplitude multiplies large one-body matrix elements in Eq. (11). Furthermore, the sensitivity is enhanced by the cross terms between large and small components in the expression for the transition rates of Eqs. (5) and (7).

Although the 3^- transition is third forbidden, its

TABLE VII. Transition rates for different nuclear models. We use $b=1.75$ F and the nuclear wave functions from Table IV.

	Transition rate (10^8 sec^{-1})															
	0^-				1^-				2^-				3^-			
C_P/C_A	IP	I_A	I_B	II	IP	I_A	I_B	II	IP	I_A	I_B	II	IP	I_A	I_B	II
−8	6.45	8.09	4.73	4.81	4.69	4.25	2.53	2.36	39.8	32.2	25.8	22.7	0.187	0.163	0.196	0.182
−4	5.18	6.46	3.83	3.91					35.0	28.3	22.7	20.0				
0	4.04	5.01	3.01	3.10					30.9	24.9	20.0	17.6				
4	3.04	3.74	2.30	2.38					27.6	22.0	17.8	15.6				
8	2.19	2.66	1.68	1.76					25.0	19.8	16.0	14.1				
12	1.47	1.76	1.16	1.23					23.1	18.1	14.6	12.9				
16	0.900	1.05	0.735	0.795					21.9	16.9	13.7	12.0				
20	0.467	0.521	0.406	0.455					21.5	16.3	13.2	11.6				
24	0.175	0.175	0.174	0.209					21.8	16.3	13.2	11.6				
28	0.0234	0.0134	0.0392	0.0577					22.8	16.9	13.6	11.9				
32	0.0126	0.0352	0	0					24.5	18.0	14.4	12.6				
36	0.142	0.241	0.0584	0.0377					27.0	19.7	15.7	13.8				

[22] L. R. B. Elton, *Nuclear Sizes* (Oxford University Press, London, 1961).

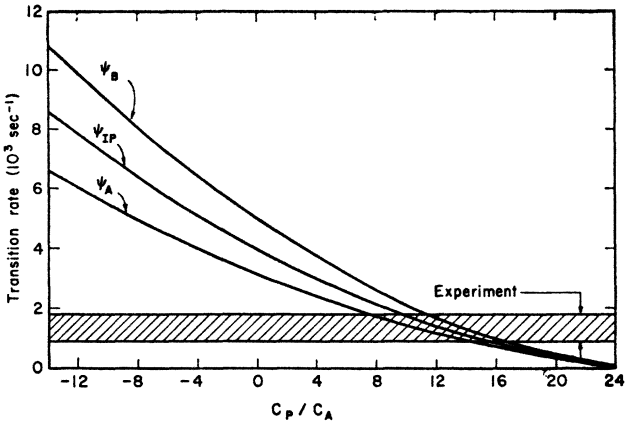

FIG. 3. Dependence of C_P on the small component of the nuclear wave function for muon capture in O^{16}. The experimental error includes both the Columbia and Berkeley data as given in Table I.

rate is 5% of the 1^- case, which is first forbidden. The high-momentum transfer in muon capture makes the forbidden transitions more important than in beta decay, for which the comparable forbidden transitions would be negligible.

V. COMPARISON WITH EARLIER WORK

It is interesting to look at the earlier works and compare them with our results. Beltrametti and Radicati have computed the matrix elements for capture in O^{16}, but they do not present the transition rates.[23] Duck does not present his rates for the $0^+ \rightarrow 0^-$ transition, but he computes $0^-/1^-$, the ratio of the $0^+ \rightarrow 0^-$ transition to the $0^+ \rightarrow 1^-$ transition.[3] It is difficult to compute the $0^+ \rightarrow 0^-$ transition from data given in Duck's paper, since there are disagreements in sign in the two publications of his work (e.g., see the phases of the wave functions and definitions of the coupling constants given in these two references). However, we can compare calculations by computing the $0^-/1^-$ ratio, using the Morita-Fujii method. Table VIII compares the results of Duck and of Ericson *et al.* with our work. Our numbers are much higher than those of Duck, but

TABLE VIII. Comparison of the transition-rate ratio, $0^-/1^-$, with oscillator length $b=1.56$ F and with the Elliott and Flower wave functions. The muon wave function is set equal to an average value in the radial integral, and F, the small component of the muon wave function, equals zero.

	C_P/C_A		
	−8	0	+8
Duck[a]	1.8	1.4	0.66
Ericson *et al.*[b]	2.4	1.5	0.86
This work	2.5	1.6	0.94

[a] Reference 3, Table 4b and 4c.
[b] Reference 2, Table III.

[23] E. G. Beltrametti and L. A. Radicati, Nuovo Cimento 11, 793 (1959).

TABLE IX. Comparison of transition rates using the Elliott and Flower wave functions.

	0^- (10^3 sec^{-1})			1^- (10^3 sec^{-1})	2^- (10^3 sec^{-1})		
$C_P/C_A=$	−8	0	+8		−8	0	+8
Ericson *et al.*[a]	8.34	5.16	2.77	3.98	29.9	23.0	18.3
This work[b]	8.09	5.01	2.66	4.25	32.2	24.9	19.8

[a] Reference 2, Table III. They use $b=1.80$ F.
[b] We use $b=1.75$ F.

we agree within 10% with Ericson *et al.* Our agreement with Ericson *et al.* is also good when we compare the absolute rates shown in Table IX. The small disagreement could be attributed to a different treatment of the lepton problem and the use of slightly different coupling constants. The discrepancy with Duck's work is not understood.

VI. ANALYSIS OF CALCULATION

A measurement of the $0^+ \rightarrow 0^-$ transition rate does not determine C_P uniquely. Figure 4 shows the transition rate as a function of C_P for nuclear model I_B, and there are two values of C_P which give agreement with the experimental value. When the C^{12} data given in Fig. 2 are used, the higher value can be excluded. The transition rate into the 0^- state is very sensitive to the small component of the nuclear wave function; as a result, we cannot accurately compute C_P until the nuclear wave functions are known more accurately. Also, the two experimental measurements of the 0^- rate are outside each other's experimental error. From our analysis of the experimental data for capture into the 0^- state, we conclude $5<C_P/C_A<20$, as shown in Fig. 3. This agrees with the theoretical value of $C_P/C_A \approx 7$ predicted by Goldberger and Treiman. The results are valid only if the induced pseudo-tensor term C_T is zero, because the introduction of another unknown C_T would lead to more doubtful conclusions in the present state of the experimental evidence and of the nuclear model.

The disagreement between theory and experiment for capture into the 1^- and 2^- states can probably be attributed to the many admixtures present in the wave

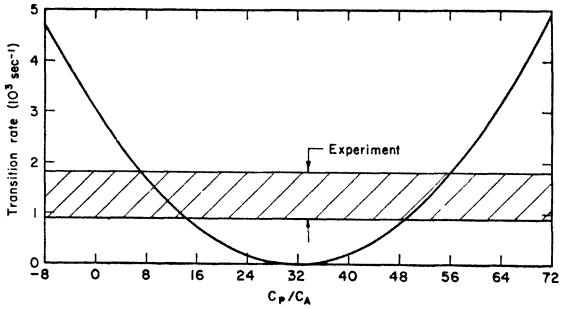

FIG. 4. Muon-capture rate in O^{16}

functions. As shown for the 0^- rate, which has only one small component, transition rates are very sensitive to the small admixtures. No conclusions can be drawn from the 1^- transition, since the rates computed by the Elliott and Flower wave functions disagree strongly with the rate computed from the Gillet and Vinh Mau wave functions, and both rates are higher than the experimental value. The 2^- transition rate does not seem to depend strongly on the nuclear model, and two calculations of this rate are in fair agreement. However, the computed rate does not agree with experiment for any value of C_P. As C_P is increased, the computed rate goes through a minimum of 1.2×10^4 sec^{-1} for $C_P/C_A \approx 22$, but this value is still higher than the measured value of 0.63×10^4 sec^{-1}.

The 3^- transition rate is so small that it has not been observed yet. However, it does not depend on C_P, so a measurement would provide a check of the wave function.

VII. CONCLUSIONS

We have computed C_P, the pseudoscalar coupling constant, from the muon capture rate in O^{16}. The calculation does not give a precise value of the pseudoscalar coupling constant because of the uncertainties in the nuclear wave function and the muon interaction. Several things can be done to improve the situation. First, an accurate nuclear wave function must be found for N^{16}. Cabibbo has suggested[24] that the amplitude for the small components could be found by using the wave functions to compute the electromagnetic transitions in N^{16}. With an accurate wave function, the coupling constant should be easy to find from this transition rate. Next, there is the question of the induced pseudotensor and induced scalar coupling constants. At present there are not enough experimental data to justify a search for these terms, and we must assume that they are zero to simplify the calculations. However, if they are present they could seriously affect the calculation of muon-capture rates. Thus far, most calculations for muon-capture rates have used a free parameter C_P and the other possible parameters C_S and C_T have been neglected. The absence of these terms could be ascertained by observing muon-capture transitions in which their matrix elements would be large compared with other terms in the Hamiltonian. For instance, a $0^+ \rightarrow 0^+$ transition would be useful for finding the C_S term because the axial-vector part of the Hamiltonian cannot contribute to the transition.

In gathering more experimental data, one must be careful to measure the muon-capture rates in those nuclei with wave functions that are reasonably well known. For this reason, the transitions $Mg^{24} \rightarrow Na^{24*}$ and $Ti^{48} \rightarrow Sc^{48*}$ have been suggested by Rasmussen.[25] Using the Nilsson model, Mang[26] has developed wave functions for Mg^{24}, and McCullen *et al.*[27] have published wave functions for Ti^{48}. At present the $Mg^{24} \rightarrow Na^{24}$ transition looks most promising, because the excited states in Na^{24} are well known and these states must be known before an experiment can be planned to measure the transition rate. The $Ti^{48} \rightarrow Sc^{48}$ transition is experimentally difficult at the moment because of the uncertainty in the excited states of Sc^{48}. There has been very little experimental investigation of Sc^{48} even though the energy levels have been predicted by McCullen *et al.*[27] and the spins of the levels have been predicted by Rasmussen.[28] If the highest excited states of Sc^{48} have $J^P=0^+$ and 1^+, as indicated by Rasmussen, this nucleus may be useful for a muon-capture experiment.

Another approach for obtaining the coupling constants has been suggested by Foldy and Walecka.[29] They obtain the nuclear matrix elements empirically from electron scattering data, and thereby avoid the uncertainties inherent in obtaining the nuclear wave functions from energy levels. They have used this approach to compute the coupling constants from the total capture rates, i.e., the capture into all final states; but they found that these rates are not sensitive to the coupling constants. However, this technique could be very useful in computing the partial transition rates, which are sensitive to the coupling constants, as we have shown.

ACKNOWLEDGMENTS

The authors wish to thank Professor John Rasmussen and Professor Emilio Segrè for their support. We thank Dr. M. Morita for assisting in checking our calculations and Dr. Torlief Ericson for informing us of his results. One of us (V. G.) wishes to thank the Nuclear Chemistry Department at the Lawrence Radiation Laboratory for its hospitality. We also thank the Computer Group at the Lawrence Radiation Laboratory for the time they made available on the IBM 7094.

APPENDIX

Detail of the Calculation of the Transition Rate

The calculation of the capture rate into the 0^- state of N^{16} begins with the evaluation of the matrix elements $\langle p\|\Xi^{(i)}\|h\rangle$. Using the nuclear model I_B, we evaluate these matrix elements for the particle-hole pairs $2s_{1/2}1p_{1/2}$ and $1d_{3/2}1p_{3/2}$. With $u=0$, $v=k$, and $\kappa=1$, the nonzero

[24] Nicola Cabibbo (private communication).

[25] John O. Rasmussen, Jr. (private communication).
[26] Hans J. Mang (private communication).
[27] J. D. McCullen, B. F. Bayman, and L. Zamick, Phys. Rev. 134, B515 (1964).
[28] J. O. Rasmussen and Y. E. Kim, in Chemistry Division Annual Report, Lawrence Radiation Laboratory Report UCRL-11213, 1963, p. 25 (unpublished).
[29] L. L. Foldy and J. D. Walecka, Nuovo Cimento 34, 1026 (1964).

matrix elements are

$$\langle 2s_{1/2}\|\Xi^{(2)}\|1p_{1/2}\rangle=\langle 2s_{1/2}\|\mathfrak{D}_{110}(\hat{r},\boldsymbol{\sigma})\|1p_{1/2}\rangle \times\Big[S_{110}(1,-1)\int_0^\infty u_{2,0}g_1G_{-1}u_{1,1}r^2dr -S_{110}(-1,+1)\int_0^\infty u_{2,0}f_1F_{-1}u_{1,1}r^2dr\Big].$$

Using $b=1.75$ F, $q=93.5$ MeV/c, and the Hermite-Gauss numerical integration procedure, we obtain

$$\langle 2s_{1/2}\|\Xi^{(2)}\|1p_{1/2}\rangle =(3/8\pi^2)^{1/2}[-(\tfrac{2}{3})^{1/2}(-8.01)-(\tfrac{2}{3})^{1/2}(0.181)]=+1.25;$$

in the same way we compute

$$\langle 1d_{3/2}\|\Xi^{(2)}\|1p_{3/2}\rangle =(\sqrt{3}/2\pi)[-(\tfrac{2}{3})^{1/2}(14.68)-(\tfrac{2}{3})^{1/2}(-0.840)]=-3.11,$$

$$\langle 2s_{1/2}\|\Xi^{(6)}\|1p_{1/2}\rangle =(-)^{1+1/2+1/2}(6)^{1/2}\sum_{l'=0,2}\langle 0\|\mathfrak{D}_{000}(\hat{r})\|l'\rangle\begin{Bmatrix}1/2 & 1/2 & l'\\ 1 & 1 & 1/2\end{Bmatrix} \times\Big[S_{000}(-1,-1)\int_0^\infty u_{2,0}f_1G_{-1}D_{l'}u_{1,1}r^2dr +S_{000}(1,1)\int_0^\infty u_{2,0}g_1F_{-1}D_{l'}u_{1,1}r^2dr\Big],$$

$$D_2=(2)^{1/2}(d/dr-1/r),$$

$$D_0=-(d/dr+2/r),$$

$$\langle 2s_{1/2}\|\Xi^{(6)}\|1p_{1/2}\rangle =(6)^{1/2}(8\pi^2)^{-1/2}((6)^{-1/2})[\sqrt{2}(-7996)+(-\sqrt{2})(66.1)] =-1283,$$

$$\langle 1d_{3/2}\|\Xi^{(6)}\|1p_{3/2}\rangle =(-)^{1+1/2+3/2}(6)^{1/2}(2\pi)^{-1}(2\sqrt{3})^{-1} \times[\sqrt{2}(-1.38\times10^4)+(-\sqrt{2})(231)]=+2233,$$

$$\langle 2s_{1/2}\|\Xi^{(7)}\|1p_{1/2}\rangle =\langle 2s_{1/2}\|\mathfrak{D}_{110}(\hat{r},\boldsymbol{\sigma})\|1p_{1/2}\rangle \times\Big[S_{000}(-1,-1)\int_0^\infty u_{2,0}D_+f_1G_{-1}u_{1,1}r^2dr +S_{000}(1,1)\int_0^\infty u_{2,0}D_+g_1F_{-1}u_{1,1}r^2dr\Big] =(3/8\pi^2)^{1/2}[\sqrt{2}(1535)+(-\sqrt{2})(-3.83)]=424.2,$$

$$\langle 1d_{3/2}\|\Xi^{(7)}\|1p_{3/2}\rangle =(\sqrt{3}/2\pi)[\sqrt{2}(-3034)+(-\sqrt{2})(-29.6)]=-1171,$$

$$\langle 2s_{1/2}\|\Xi^{(8)}\|1p_{1/2}\rangle =(3/8\pi^2)^{1/2}[\sqrt{2}(1535)-(-\sqrt{2})(-3.83)]=422.1,$$

$$\langle 1d_{3/2}\|\Xi^{(8)}\|1p_{3/2}\rangle =(\sqrt{3}/2\pi)[\sqrt{2}(-3034)-(-\sqrt{2})(-29.6)]=-1194.$$

From Table IV we find

$$X_{2s1p}=0.999,$$
$$X_{1d1p}=0.055.$$

Using Eqs. (8) and (11), we compute

$$\mathfrak{M}^{(2)}=\langle f\|\Xi^{(2)}\|0\rangle =(0.999)(1.25)+(0.055)(-3.11) =1.08,$$
$$\mathfrak{M}^{(6)}=-1159,$$
$$\mathfrak{M}^{(7)}=359,$$
$$\mathfrak{M}^{(8)}=356.$$

Letting $C_P=7C_A$, we obtain for the coupling constants in natural units

$$C^{(2)}=3.55\times10^{-12},$$
$$C^{(6)}=-1.93\times10^{-15},$$
$$C^{(7)}=5.58\times10^{-16},$$
$$C^{(8)}=-3.91\times10^{-15}.$$

These matrix elements and coupling constants are substituted into Eq. (7) to give

$$|\langle f|H|0\rangle|_{\mathrm{av}}{}^2=1.17\times10^{-23}.$$

With a value of $q=183$ (natural units), we find the transition rate from Eq. (5) to be

$$\lambda=(2\pi)(1.17\times10^{-23})(183)^2(0.994)(1.288\times10^{-21})^{-1} =1.90\times10^3\ \mathrm{sec}^{-1},$$

where we have used $\hbar/m_ec^2=1.288\times10^{-21}$ sec.